

Dark dynamic acousto-optic ring lattices for ultracold atoms

N. Houston, E. Riis, A. S. Arnold

SUPA, Dept. of Physics, University of Strathclyde, Glasgow G4 0NG, UK

Abstract: We demonstrate the optical generation of dynamic dark optical ring lattices, which do not require Laguerre-Gauss beams, large optical coherence lengths or interferometric stability. Simple control signals lead to spatial modulation and reproducible rotation, offering manifold possibilities for complex dynamic ring lattices. In conjunction with a magnetic trap, these scanned 2D intensity distributions from a single laser beam will enable precision trapping and manipulation of ultracold species using blue-detuned light. The technique is ideal for azimuthal ratchet, Mott insulator and persistent current experiments with quantum degenerate gases.

© 2018 Optical Society of America

OCIS codes: (020.7010) Trapping; (230.1040) Acousto-optical devices

References and links

1. E. A. Hinds and I. G. Hughes, "Magnetic atom optics: mirrors, guides, traps, and chips for atoms," *J. Phys. D* **32**, R119-R146 (1999); C. S. Adams and E. Riis, "Laser cooling and trapping of neutral atoms," *Prog. Quant. Electr.* **21**, 1-79 (1997); Ultracold atom network, <http://ucan.physics.utoronto.ca>.
2. S. Gupta, K. W. Murch, K. L. Moore, T. P. Purdy and D. M. Stamper-Kurn, "Bose-Einstein condensation in a circular waveguide," *Phys. Rev. Lett.* **95**, 143201 (2005); A. S. Arnold, C. S. Garvie and E. Riis, "Large magnetic storage ring for Bose-Einstein condensates," *Phys. Rev. A* **73**, 041606(R) (2006).
3. C. Ryu *et al.*, "Observation of persistent flow of a Bose-Einstein condensate in a toroidal trap," *Phys. Rev. Lett.* **99**, 260401 (2007).
4. D. S. Naik, S. R. Muniz and C. Raman, "Metastable Bose-Einstein condensate in a linear potential," *Phys. Rev. A* **72**, 051606(R) (2005).
5. A. Hopkins, B. Lev, and H. Mabuchi, "Proposed magnetoelectrostatic ring trap for neutral atoms," *Phys. Rev. A* **70**, 053616 (2004).
6. P. F. Griffin, E. Riis, and A. S. Arnold, "Smooth inductively coupled ring trap for atoms," *Phys. Rev. A* **77**, 051402(R) (2008).
7. S. Hofferberth *et al.*, "Radiofrequency-dressed-state potentials for neutral atoms," *Nature Phys.* **2**, 710-6 (2006); W. H. Heathcote *et al.*, "A ring trap for ultracold atoms in an RF-dressed state," *New J. Phys.* **10**, 043012 (2008).
8. E. Jané, G. Vidal, W. Dür, P. Zoller, J. I. Cirac, "Simulation of quantum dynamics with quantum optical systems," *Quantum Inform. Comp.* **3**, 15-37 (2003).
9. R. P. Feynman, "Simulating physics with computers," *Int. J. Theor. Phys.* **21**, 467 (1982).
10. A. Kay, J. K. Pachos and C. S. Adams, "Graph-state preparation and quantum computation with global addressing of optical lattices," *Phys. Rev. A* **73**, 022310 (2006).
11. M. Greiner, O. Mandel, T. Esslinger, T. W. Hänsch and I. Bloch, "Quantum phase transition from a superfluid to a Mott insulator in a gas of ultracold atoms," *Nature* **415**, 39-44 (2002).
12. F. S. Cataliotti *et al.*, "Josephson junction arrays with Bose-Einstein condensates," *Science* **293**, 843-846 (2001).
13. L. Plaja and J. San Román "Dynamics of the formation of bright solitary waves of Bose-Einstein condensates in optical lattices," *Phys. Rev. A* **69**, 063612 (2004); L. Amico, A. Osterloh and F. Cataliotti, "Quantum many particle systems in ring-shaped optical lattices," *Phys. Rev. Lett.* **95**, 063201 (2005); A. M. Rey *et al.*, "Entanglement and the Mott transition in a rotating bosonic ring lattice," *Phys. Rev. A* **75**, 063616 (2007).
14. R. Ozeri, L. Khaykovich and N. Davidson, "Long spin relaxation times in a single-beam blue-detuned optical trap," *Phys. Rev. A* **59**, 1750 (1999).
15. N. Chattrapiban, E. A. Rogers, I. V. Arakelyan, R. Roy and W. T. Hill, "Laser beams with embedded vortices: tools for atom optics," *J. Opt. Soc. Am. B* **23**, 94 (2006).
16. S. Franke-Arnold *et al.*, "Optical ferris wheel for ultracold atoms," *Opt. Express* **15**, 8619 (2007).

17. V. Boyer, C. M. Chandrashekar, C. J. Foot and Z. J. Laczik, "Dynamic optical trap generation using FLC SLMs for the manipulation of cold atoms," *J. Mod. Opt.* **51**, 2235 (2004); V. Boyer *et al.*, "Dynamic manipulation of Bose-Einstein condensates with a spatial light modulator," *Phys. Rev. A* **73**, 031402(R) (2006).
18. R. Onofrio *et al.*, "Surface excitations of a Bose-Einstein condensate," *Phys. Rev. Lett.* **84**, 810 (2000).
19. K. Bongs *et al.*, "Coherent evolution of bouncing Bose-Einstein condensates," *Phys. Rev. Lett.* **83**, 3577 (1999).
20. K. W. Madison *et al.*, "Vortex formation in a stirred Bose-Einstein condensate," *Phys. Rev. Lett.* **84**, 806 (2000).
21. S. Schwartz, M. Cozzini, C. Menotti, I. Carusotto, P. Bouyer and S. Stringari, "One-dimensional description of a Bose-Einstein condensate in a rotating closed-loop waveguide," *New J. Phys.* **8**, 162 (2006).
22. S. K. Schnelle, E. D. van Ooijen, M. J. Davis, N. R. Heckenberg and H. Rubinsztein-Dunlop, "Versatile two-dimensional potentials for ultra-cold atoms", *Opt. Express* **16**, 1405 (2008).
23. M. G. Boshier, private communication.
24. R. Gommers, V. Lebedev, M. Brown and F. Renzoni, "Gating ratchet for cold atoms," *Phys. Rev. Lett.* **100**, 040603 (2008), and references therein.
25. W. Petrich, M. H. Anderson, J. R. Ensher and E. A. Cornell, "Stable, tightly confining magnetic trap for evaporative cooling of neutral atoms," *Phys. Rev. Lett.* **74**, 3352 (1995). A. S. Arnold, "Adaptable-radius, time-orbiting magnetic ring trap for Bose-Einstein condensates," *J. Phys. B* **37**, L29 (2004);
26. N. Houston, E. Riis and A. S. Arnold, in preparation.
27. D. R. Scherer, C. N. Weiler, T. W. Neely and B. P. Anderson, "Vortex formation by merging of multiple trapped Bose-Einstein condensates," *Phys. Rev. Lett.* **98**, 110402 (2007).

1. Introduction

Laser cooling and the subsequent attainment of quantum degenerate gases has enabled exquisite control over atoms. Coherent atom-optical manipulation of coherent atomic gases, typically with magnetic fields and/or far-detuned lasers, is now a worldwide phenomenon [1]. There are a plethora of available atom trapping geometries and rings are of particular interest because they enable precision Sagnac interferometry and detailed studies of superfluidity, plus the periodic boundary conditions afford simple modeling of the system.

Bose-condensed atoms have recently been obtained in magnetic ring geometries with 1 – 50mm diameters [2] and persistent currents [3] have been observed in a small-scale condensate ring trap [4]. Ultracold atom ring traps based on electrostatic potentials [5] and induced currents [6] have also been proposed, and RF dressed rings have been experimentally realised [7].

Confinement within optical lattice geometries offers further possibilities; potentially as a tool for performing universal simulation of quantum dynamics [8], and for realisation of Feynman's ideas of quantum logic [9], thus forming a promising basis for quantum computation [10]. Optical lattices enable condensed matter physics investigations, such as the quantum phase transition from superfluidity to Mott insulator [11] and the realisation of Josephson junction arrays [12]. The combination of rings and lattices to form ring lattices with rotational symmetry and periodic boundary conditions is particularly beneficial for e.g. studies of solitons, quantum many particle systems, entanglement, Mott transitions and persistent currents [13].

Ring lattice potentials utilise far-detuned optical dipole beams, which can be clearly divided into 'bright' or 'dark' lattices: atoms are attracted to dark (bright) spatial regions of the time-averaged optical potential if one uses light blue-detuned (red-detuned) from an atomic resonance. Blue-detuned light is preferable for optical manipulation, as atoms trapped in low intensity light experience lower photon scattering (i.e. heating) rates, energy level shifts, and light assisted collisional losses [14]. Blue-detuned ('dark') trapping is likely to be necessary for lattice based quantum computation, to ensure robustness against decoherence [10].

Dark optical ring lattices [15] have been previously realised using copropagating superpositions of Laguerre-Gauss (LG) laser beams [16]. Complex optics (spatial light modulators, SLMs) were used to generate separate static LG beams, which were then frequency shifted by independent acousto-optic modulators (AOMs). For a dynamic lattice the LG beams must be recombined on a beamsplitter, leading to power loss and a requirement for interferometric relative beam stability to ensure reproducible long term experiments. An alternative way to produce

smooth time-dependent lattices is to update dynamically the SLM pattern; however update rates tend to be slow, and for the faster binary SLMs additional control algorithms must also be used, due to SLM interframe artifacts [17].

Bright ring lattices can be directly generated with AOMs. The acoustic mode frequency and amplitude in an AOM determine the beam deflection angle and intensity respectively, allowing spatial control [18]. By scanning the position of a laser beam in one or two dimensions it is possible to create a BEC mirror [19], condensate surface excitations and multiple-site traps [18], or ‘stir’ a condensate to produce vortices [20]. Two-dimensional *bright* ring lattice potentials using scanned red-detuned laser beams have been suggested [21], optically realised [22] and experimentally implemented for storing and splitting Bose-Einstein condensates [23].

Here we utilize two-dimensional AOM beam scanning [18, 22, 23] to optically demonstrate simple *dark* optical ring lattice potentials for use with ultracold atoms or BECs, without the need for relative laser beam phase coherence required in reference [16]. In BEC experiments using destructive imaging, the requirement of a ring lattice with a well defined shot-to-shot angular phase is crucial and our potentials can be reproducibly rotated around the beam axis and also spatially modulated. Moreover, if additional confinement is provided by a magnetic field (section 4), a blue-detuned realization of the dark ring lattice will be essentially decoherence free [10] and highly adaptable – ideal for Mott insulator [11], persistent current [3] and azimuthal ratchet [24] experiments involving quantum degenerate gases. We will discuss the ring lattice theory, describe the experiment, then place our results in an atom optics context.

2. Theory

We consider ring-lattice potentials based on a laser beam following a 2D path of the form:

$$\{x, y\} = R\{\sin(\omega_1 t), \cos(\omega_1 t)\} \quad (1)$$

where $R(\omega_2 t + \phi)$ is an arbitrary function with period $2\pi/\omega_2$ (i.e. R is comprised of Fourier components at angular frequencies that are integer multiples of ω_2). The overall period of the parametric function is $T = 2\pi/\text{gcd}(\omega_1, \omega_2)$ (gcd =greatest common divisor). Equation (1) forms a large family of rotationally symmetric ‘flower like’ curves (Figure 1) defined by the Fourier components of R . The frequency ratio ω_2/ω_1 is related to the number of ‘petals’ in the curve and any curve can be directly rotationally modulated using the overall phase of R , i.e. ϕ .

Half integer values of ω_2/ω_1 produce curves with a ring lattice profile (Figure 1(a)), integer values of ω_2/ω_1 produce curves which, when combined with a magnetic quadrupole potential (section 4) create a hybrid magneto-optic ring lattice (Figure 1(d)) and it is also possible to make patterns with broken angular symmetry for ring ratchet experiments (Figure 1(e)). Additionally, by adjusting the phase ϕ of the amplitude modulation R during the circular beam modulation (at ω_1), angular rotation or angular modulation of the curve can be achieved.

Laser beam deflection from an AOM is proportional to the RF drive frequency. The deflection can be modulated by altering the drive RF frequency, which can be achieved by varying

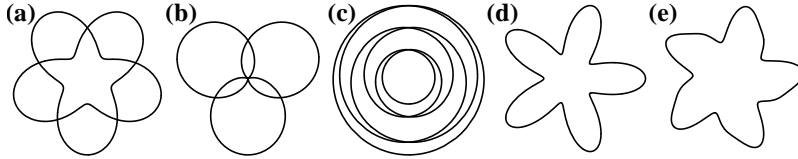


Fig. 1. Parametric curves described by Eq. (1) with $R = A + B \sin \omega_2 t$ and $\{A/B, \omega_2/\omega_1\}$ set to: $\{1/2, 5/2\}$ (a); $\{1, 3/2\}$ (b); $\{1/2, 1/6\}$ (c); $\{1/2, 5\}$ (d). In (e) the angular symmetry of the lattice is broken using $R = A(1 + \sin(\omega_2 t)/5 + \sin(2\omega_2 t)/20)$.

the voltage driving a voltage controlled oscillator (VCO). Thus AOM deflection is synchronised to the VCO input voltage. If a laser beam is passed through two perpendicular AOMs, with corresponding VCOs driven by the parametric signal Eq. (1), the variation in the vertical and horizontal deflection angles will cause the beam to trace out the corresponding parametric curves. If this variation is rapid compared to typical atomic velocities, ultracold species will effectively experience only the time-averaged geometry of the beam trace [25], allowing both trapping and spatial control of atoms or BECs within the scanned beam.

3. Experiment

The design used to generate the required VCO control signals is shown schematically in Figure 2. The circuit is able to operate from a single ‘master’ synthesized signal generator (SSG_M , e.g. Agilent 33220A or SRS DS345) by taking advantage of the 10MHz clock output, to synchronise a second ‘slave’ SSG_S (or control circuitry [26]). SSG_M is used for radial modulation of the circular beam path provided by SSG_S . We have used analogue multipliers because the amplitude modulation function of a typical SSG has limited bandwidth.

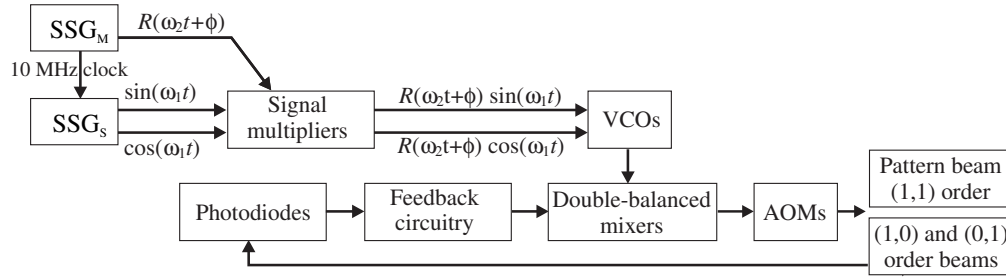


Fig. 2. The signal generation circuit is based on two synthesized signal generators (SSG). Our slave synthesizer SSG_S is actually a custom-made circuit based on low-cost ICs [26].

The multiplier outputs (Eq. 1) are then fed to two independent VCOs to provide the RF signals for driving two 110MHz AOMs. Voltage controlled attenuators (VCAs) or double-balanced mixers are then used for control over RF power, and thus beam intensity, during the beam scan. Our base frequency is currently set to $\omega_1 = 2\pi \times 10\text{kHz}$ (a subharmonic of the SSG_M clock) for convenience, however with sufficient VCO bandwidth, this could easily be increased by more than a factor of ten.

Figure 3 shows the experimental setup. A helium-neon laser beam is focused through two perpendicular AOMs, which are placed close to each other to minimise output distortion and scan asymmetry. Each AOM produces a spread of diffractive orders which results in a grid of diffracted beams at the output.

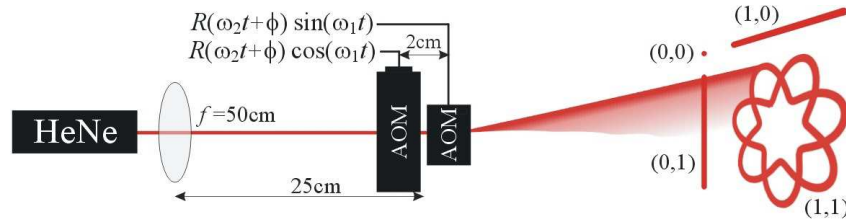


Fig. 3. Experimental setup for generation of optical ring lattices. Synchronised variation in AOM deflection angles causes the beam to trace out the ring lattice shown.

Figure 4 shows experimental results for 5-site optical ring lattices realised using this technique, as well as comparison to 10-parameter 2D least-squares fits from a simple theoretical model based on a Gaussian beam with x and y beam waists of w_x and w_y respectively, scanned in the xy plane yielding a time-averaged intensity:

$$\overline{I(x,y)} = \frac{I_0 s \omega_1}{2\pi} \int_0^{\frac{2\pi}{s\omega_1}} \exp[-2(x-x_r(t))^2/w_x^2 - 2(y-y_r(t))^2/w_y^2] dt; \quad (2)$$

where $\{x_r, y_r\} = \{x_0 - (r_x + A_x \sin(5s\omega_1 t + \phi)) \sin(\omega_1 t), y_0 - (r_y + A_y \sin(5s\omega_1 t + \phi)) \cos(\omega_1 t)\}$ is the position of the center of the scanned beam at time t . The parameter s is set to $\frac{1}{2}$ or 1 for a closed optical ring lattice (cf. Fig. 1 (a)) or open optical ring lattice (cf. Fig. 1 (d)) respectively.

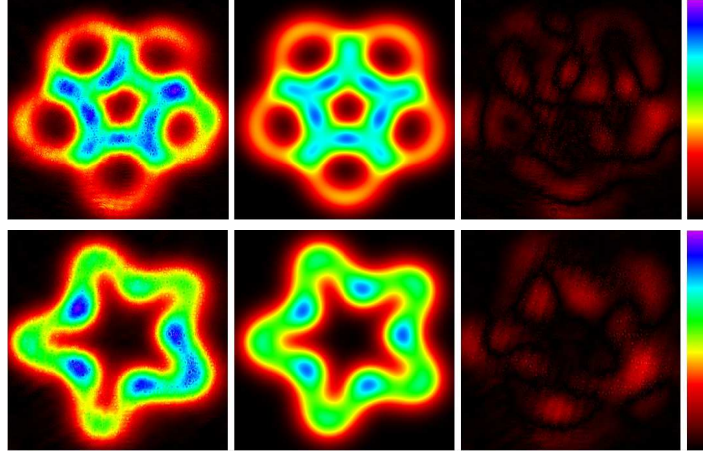


Fig. 4. Experimental relative intensity distributions (area $\approx (4\text{mm})^2$, exposure 1 ms), corresponding least-squares theoretical fits using Eq. 2 and fit residues. Click here for optical lattice movies comparing experimental and theoretical rotation and amplitude modulation. The static laser beam has a waist (e^{-2} radius) $\approx 300\ \mu\text{m}$.

As the contribution to the time-averaged intensity is inversely proportional to the velocity of the center of the scanned beam, there is a radial intensity gradient due to the deflected beam spending longer in the center of the pattern. This gradient does not affect the quality of the trapping potential for e.g. Mott insulator experiments, as long as the pattern has a high level of rotational symmetry. It is therefore important to scan a dipole beam with an aspect ratio as close as possible to 1, with a stable beam intensity during the scan process. To this end we have implemented a feedback mechanism (‘noise-eater’) to the VCA control signals based on error signals generated from the unused (1,0) and (0,1) AOM deflection orders (Fig. 3). The advantage of feedback, as opposed to recorded feedforward [22], is that it immediately adapts to beam intensity noise due to environmental changes or changes to the amplitude modulation function. Although high bandwidth is required for feedback, we have already reduced intensity amplitude noise to 5% rms, and anticipate future improvements.

4. Atom optics

Whilst there has been growing theoretical interest in ring lattices [13], the closest experiment to a dark BEC ring lattice has consisted of three sites produced by variable intensity light traversing a static mechanical aperture [27]. The azimuthal and central barriers of this 3-site

ring lattice must be altered together. In contrast the azimuthal and central barrier of our N -site optical potential can be altered independently. Additionally, as the azimuthal lattice angle is purely controlled by the phase ϕ of the VCO amplitude modulation, the ring lattice can be reproducibly rotated, even for BECs with experimental production times of minutes.

We now give a brief illustration of experimentally realistic parameters for a 5-site optical ring lattice. The scanned laser beam leads to an optical dipole trap with atomic scattering rate (Hz) and depth (J) approximately given by $S \approx \Gamma \bar{I} / (8I_S \Delta_\Gamma^2)$ and $U \approx \hbar \Gamma \bar{I} / (8\Delta_\Gamma I_S)$ respectively, where \bar{I} and $\Delta_\Gamma = (\omega - \omega_0) / \Gamma$ are the time-averaged spatial intensity and laser detuning from the atomic transition (in linewidths). A very useful, species independent parameter for blue-detuned dipole traps is $S/T = k_B / (\hbar \Delta_\Gamma)$ - the *maximum* scattering rate experienced by an atom with total energy $U = k_B T$ as a function of the dipole trap depth. For the 780 nm D2 transition in ^{87}Rb , $\Gamma = 2\pi \times 6\text{MHz}$ and $I_S = 16.7\text{W/m}^2$. If we use a dipole trap laser with wavelength $\lambda = 765\text{nm}$ ($\Delta_\Gamma \approx 1.3 \times 10^6$) we have $S/T = 0.1\text{Hz}/\mu\text{K}$. Assuming a laser waist of $w = 20\mu\text{m}$, and power $P = 400\text{mW}$, Fig. 5 illustrates the optical dipole potential, as well as its combination with a magnetic quadrupole field $\mathbf{B} = 100\text{G/cm} \{-x/2, -y/2, z\}$ for atoms in the ground state $|F = 2, m_F = 2\rangle$, yielding an adiabatic magnetic potential $U_B = \mu_B |\mathbf{B}|$ [1].

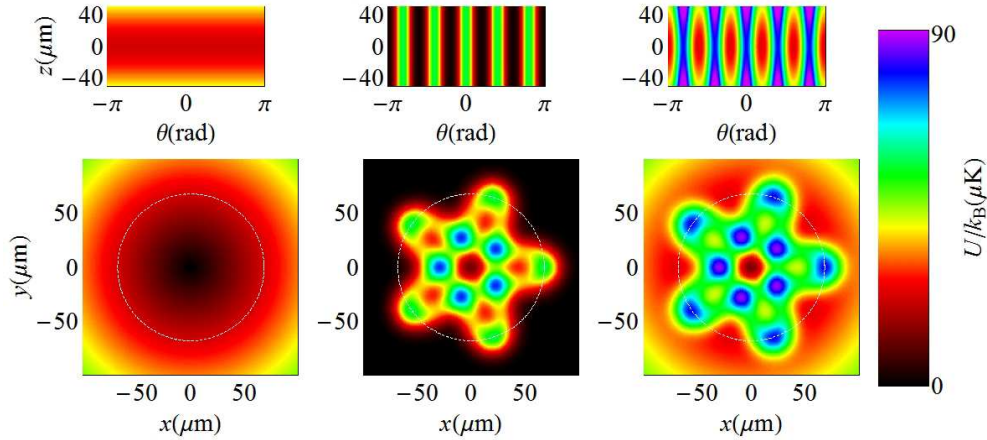


Fig. 5. Magnetic (left), optical (center) and hybrid magneto-optical potentials (right). The upper images show axial-azimuthal slices indicated by the dashed white circles.

In addition to the dramatically reduced heating rates afforded by blue-detuned (dark) dipole traps, it should be stressed [18] that dark ring lattices should greatly reduce the observed heating due to micromotion of atoms during AOM beam scan in bright dipole traps. Additionally, scattering a few photons tends to optically pump atoms into magnetically untrapped states: thus dark (bright) traps scatter more photons in the hottest (coldest) parts of the potential leading to evaporative cooling (heating).

5. Conclusions and Acknowledgments

We have experimentally obtained reproducible optical ring lattices for use with blue-detuned light, which allow controllable rotation and spatial modulation. The lattices produced are relatively insensitive to environmental conditions and do not require either LG beams, SLMs, or other complex optics. This technique could possibly be utilised for rotation of a “quantum register,” and for new forms of optical tweezing.

We gratefully acknowledge discussions with Dr. Malcolm Boshier and Dr. Ifan Hughes.